Indo. J. Chem. Sci. 13 (2) (2024)
Indonesian Journal of Chemical Science
http://journal.unnes.ac.id/sju/index.php/ijcs

Characterization and Optimization of Fe_2O_3 Extraction From Red Mud Using APDC ligan

Elli Prastyo ✉, and Yully Mulyani

Chemical Engineering Department, Institut Teknologi Petroleum Balongan, Pekandangan, Indramayu, West Java, 45216, Indonesia[1, 2]

Article Info

Accepted : 13-05-2024

Approved : 05-08-2024

Published : 26-08-2024

Keywords:
Extraction, Fe2O3, Ligans, Optimizing, Red Mud

Abstract

The main component contained in the red mud is Fe_2O_3 which has the potential to be used as a catalyst in chemical reactions and can be used as a Fe_3O_4 catalyst manufacture. One method that can separate ferrous metal (Fe) from Red Mud is the extraction method using a chelating agent. This study studied the extraction of Fe_2O_3 from red mud by solvent extraction method using APDC ligands under various concentration. The variables studied are pH optimization, ligand concentration and extraction time. Analysis of red mud extraction results using FTIR, XRF, and XRD on various variables. Determination of the maximum wavelength of complex compounds formed between Fe(III) ions and ammonium pyrrolydine dithiocarbamate (APDC) ligands with pH variations of 1, 2, 3, 4, 5, and 6 in the wavelength range of 200 – 450 nm. The resulting complex compound is yellow and obtained a maximum wavelength of 347 nm. The greatest value of Fe_2O_3 absorbance is obtained at pH 1. The concentration of APDC ligands on the extraction of Fe-APDC complex compounds reached optimum conditions at a concentration of 0.5 mM with an optimum extraction time of 5 min. The FTIR spectrum formed in the Fe_2O_3 compound from the extraction is shown by the presence of vibration peaks in the regions of 447 cm-1 and 524 cm-1. Analysis of XRD Fe_2O_3 extraction results from red mud showed that the dominant phase was hematite (Fe_2O_3) followed by the minor phase of SiO_2.

✉ Correspondence address:
Chemical Engineering Department, Institut Teknologi Petroleum Balongan,
Pekandangan, Indramayu, West Java, 45216, Indonesia
E-mail: fiyan.maulana48@gmail.com (choose Correspondence Style)

p-ISSN 2252-6951
e-ISSN 2502-6844

Introduction

Bauxite deposits are one of Indonesia's potential mineral resources. PT Indonesia Chemical Alumina (ICA) produces Chemical Grade Alumina (CGA), with a production capacity of 300,000 tons per year since 2014. The increased aluminum production capacity has an impact on the number of red mud that will be produced will also continue to increase. The amount of red mud ranges from 40-50% of the weight of the ore or from 1 ton of bauxite will be produced 0.8-1.5 tons of red mud (Fallah, 2013). Red mud in general is very alkaline with a pH value between 12-13. Chemically, red mud consists of the main components, one of which is Fe_2O_3 around 20-45% (Renforth, *et al*., 2012).

Red mud has characteristics such as very fine particle size (≤10 μm) and high alkalinity (pH 10.0 - 12.5) (Samal, 2021). Several studies have been carried out by utilizing red mud as a catalyst (Sushil, 2013) the material for making catalysts and supporting catalysts. Red mud contains minerals - the main minerals such as hematite (Fe_2O_3), geothite (α-FeOOH), boehmite (γ-AlOOH), quartz (SiO_2), sodalite ($Na_4Al_3Si_3O_{12}Cl$) and other minor components such as calcite ($CaCO_3$). One of the main components contained in the red mud is Fe_2O_3 or iron (III) oxide which has the potential to be used as a catalyst Fe_3O_4 with sol-gel method and test its activity for the reaction of CO_2 to methanol conversion (Singh, *et al*., 2019).

The most commonly used method to manage red mud is washing using HCl and seawater before the red mud is accommodated into a holding pond (Ardau, et al, 2013). The use of extraction methods through chelate formation is one of the good ways of binding heavy metals because it can form stable complexes (Kansal, *et al*., 2013). The separation of Fe_2O_3 from red mud has been carried out by (Ramdhani, 2016), the separation is carried out based on physical properties where it is known that the specific gravity of Fe_2O_3 is greater than that of Al_2O_3 and SiO_2. However, this separation method is not effective because Fe_2O_3 has not been completely separated so the alumina extraction process must be continued with hydrometallurgical methods that require large amounts of chemical reagents (HCl and NaOH) (Fallah, *et al*., 2013).

Extraction is carried out using a chelate agent, namely ammonium pyrrolidine dithiocarbamate (APDC) ligand which has the ability and flexibility to be able to extract complexes of more than 30 types of metals at low pH. Extraction of chelate formation using APDC ligands obtained optimum pH at pH 2. Samples with a pH of 2 provide the best metal reduction from the pH range of 1–5 (Reid, *et al*., 2017).

This study was carried out the extraction of Fe_2O_3 from red mud by solvent extraction method using APDC ligand. The solvent extraction process using APDC Ligand as a training agent is expected to bind fe^{3+} cations specifically by forming a complex that can dissolve in organic solvents. The research that will be carried out is the extraction and characterization of Fe_2O_3 metal using APDC ligands to obtain high amendments of Fe_2O_3 metal from red mud derived from PT. ICA, Tayan, West Kalimantan.

Method

The materials used in this study were red mud samples from PT Indonesia Chemical Aluminan Tayan, Sanggau Regency, West Kalimantan. The red mud taken wet is then dried and then the sample is destructed until smooth and sifted with a sieve measuring 200 mesh. Nitric acid 1 M (HNO_3) p.a, concentrated acetic acid (CH_3COOH) (analytical grade), hydrochloric acid (HCl) (analytical grade), citric acid 1 M ($C_6H_8O_7$) (analytical grade), ammonium pyrolyzine dithiocarbamate 0.1 M [$(CH_2)4CNS_2NH_4$], iron (III) chloride ($Fe(Cl)_3.6H_2O$) (analytical grade), methyl isobutyl ketone ($C_4H_9COCH_3$) (analytical grade), sodium hydroxyde 1 M (NaOH) (analytical grade), sodium acetate (CH_3COONa) (analytical grade), and sodium chloride (NaCl) (analytical grade).

The equipment used in this study is a hot plate and magnetic stirr for the manufacture of red mud solution. A set of soxhlet extraction tools for the red mud extraction process using APDC solvent. Rotary evaporators are used for purification of extraction results by evaporating solvents. Set of glass wear tools for analysis, oven for drying process, furnace for activation of active sites red mud extraction results.

Optimizing Concentration Ligans

The extraction was performed using 250 ml Erlenmeyer containing Fe^{3+} concentration of 10 ppm with a volume of 10 ml. The pH value is created at optimum pH conditions by adding HNO_3 and NaOH. An acetic buffer is added to maintain the pH of the solution. The solution was carried out the addition of 1 gram of NaCl and APDC extractants with a concentration of 0.5, 0.6, 0.7, 0.8 and 0.9 mM as much as 5 ml, then 10 ml of MIBK were added. The solution is stirred so that it is mixed homogeneously until 2 phases are formed. The organic phase is accommodated in the cuvette and then measured the absorbance using a UV-Vis spectrophotometer, a graph of the relationship between the concentration of the ligand and the absorbance is made (Lymperopoulou, *et al*., 2019).

Optimizing of Extraction Red Mud

Iron oxide extraction refers to (Nurhayati, *et al.*, 2019). The red mud sample was weighed as much as 15 grams dissolved in 1M HCl with a volume of 50 mL. The solution is stirred and heated at a temperature of 70◦C for 1 hour. The solution resulting from the heating process is filtered to separate the filtrate and residue. The residue is dried using an oven at a temperature of 150◦C until a crust forms, after drying, the precipitate is crushed to the form of a fine hill which is continued with the extraction of iron oxide at optimum conditions referring to the research (Guanghui, *et al.*, 2014) that has been modified. Extraction is carried out by introducing a sample of 10 grams into the Erlenmeyer 250 ml, the pH is made at optimum pH conditions. The extraction residue is carried out by a drying process at a temperature of 150°C followed by a calcination process of 700°C temperature. Calcined materials were characterized testing using FTIR, XRD, and XRF.

Determine of Length Wave and pH Optimizing

A solution of Fe^{3+} 10 ppm was introduced into the erlenmeyer at varying pH values of 1,2,3,4,5 and 6 through the addition of HNO_3 and NaOH. Acetic buffers are used to maintain the pH value of the solution. NaCl, 1mM APDC extractant, and MIBK are added to the 10 ppm Fe^{3+} solution and then mixed until 2 phases are formed (Nan, *et al.*, 2017). The organic phase is accommodated in a cuvette for absorbance measurements using a UV-Vis spectrophotometer.

Results and Discussion

This study was conducted to determine the character of Fe_2O_3 as a result of the extraction and calcination process of red mud obtained from Chemical Alumina West Kalimantan. The optimization process is carried out through the addition of APDC ligands by controlling the pH value at various extraction times. Fe_2O_3 characterization was performed using XRF, XRD, and FTIR analysis.

Length Wave and Optimizing of pH

This study began by determining the maximum wavelength of complex compounds formed between Fe (III) ions and ammonium pyrolydine dithiokarbamate (APDC) ligands with pH variations used pH 1; 2; 3; 4; 5 and 6. The wavelength range of 200 – 450 nm is used because the resulting complex compounds are yellow and a maximum wavelength of 347 nm is obtained. A graph of the relationship between wavelength and absorbance at pH variation can be seen in the following figure.

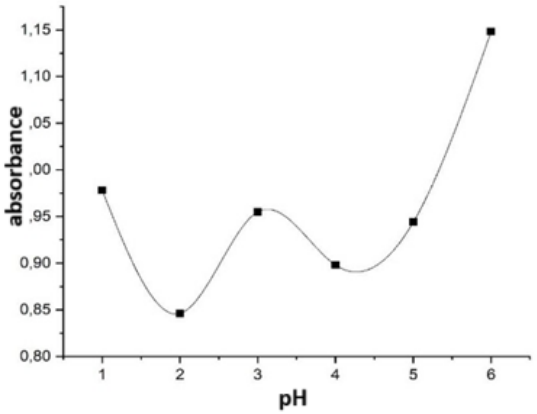

Figure 1. Relationship curve between absorbance to pH of solution

Variations in pH cause a change in the absorbance value of the Compound Fe-APDC complex. Figure 1 shows that the largest absorbance value is obtained at pH 6. The optimum pH value occurred the complexation of Fe(III) with ammonium pyrolydine dithiokarbamate (APDC) extractants. The results of the formation of the Fe-APDC complex arise from the competition between H^+ and Fe^{3+} in fighting for APDC ions.

Based on the law of reaction equilibrium, the reaction occurs a reduction in the concentration of H^+ ions, so that the reaction undergoes a shift towards the formation of the Fe-APDC chelate complex (Rayaroth, *et al.*, 2022). Figure 1 shows when pH 6 produces a high absorbance. This is because the extraction pH 6 solution has a high clarity rate, so it can affect the absorbance value. NaOH solution is added to regulate the solution to pH 6, so that there is competition between OH- and Fe^{3+} ions in binding to APDC ligands which has an impact on reducing the formation of fe-APDC chelate complexes. This is in accordance with the

opinion of (Jian, *et al*., 2013) that is, at a certain level of pH the metal will form a hydroxide that will affect the reaction. This is likely to occur competition between hydroxide ions (OH^-) from bases added with APDC ions to interact with Ni(II) ions and ni$(OH)_2$ compounds are formed, so that Ni^{2+} reacting with APDC is reduced. This is in accordance with the research of (Yanti, 2019) which states for pH 2 to pH 4 the absorption is increasing. At a pH of more than 4 absorbances are reduced due to an increase in OH concentration which causes Ni^{2+} ions to bind to OH to form $Ni(OH)_2$, but the absorbance value increases when the pH of the solution is more than 5 due to the release of OH^- ions in the solution.

Optimizing of Ligan Concentration

Ligand concentration optimization procedure to determine the concentration of APDC ligands at optimum pH with maximum wavelength. The optimum pH value was achieved at pH 1 with a wavelength of 437 nm in the previous process. The results of the observation of the curve between the absorbance of complex compounds and the concentration of APDC ligands are seen in figure 2.

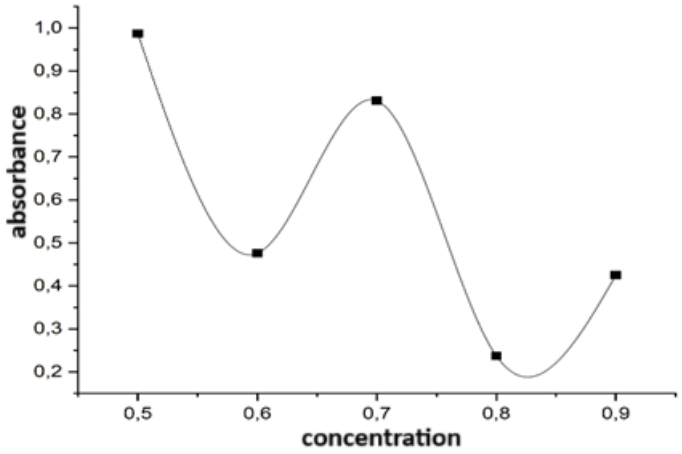

Figure 2. Relationship curve between absorbance and ligand concentration

Figure 2 shows thatAPDC ligand concentrations reach optimum at a concentration of 0.5 mM. The graph shows fluctuations from high absorbance at low concentrations then absorbances falling when concentrations are raised. This is due to the fact that metal compounds have passed reacting. The absorbance will reach the optimum price if the Metal Compound Fe (III) has reacted with the APDC ligand. It is in accordance with Lambert Beer's law that absorbance is directly proportional to the concentration of the compound. As for the occurrence of a decline. The value of the peak current after the maximum peak current due to the inhibition of ligand adsorption due to free ligand competition (Jian, *et al*., 2013). With the increase in the concentration of ligands makes the adsorption of metal complexes decrease (Yanti, 2019).

Optimizing of Extraction Time

The purpose of this process is to determine the optimal extraction time of the Fe-APDC complex compound. The extraction time is calculated starting from the addition of organic solvent methyl iso butyl ketone (MIBK). Observational data from the research results of the relationship between absorbance and extraction time of Fe-APDC complex compound formation are presented in figure 3.

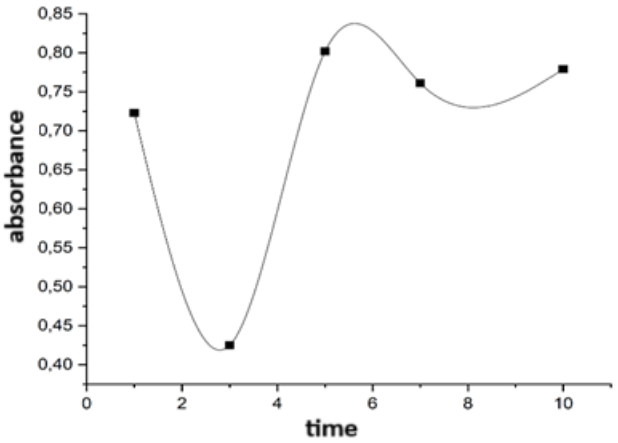

Figure 3. Relationship curve between absorbance and extraction time

Figure 3 shows that the extraction time affects the formation of Fe-APDC complex compounds, so it will affect the absorbance value. The increasing extraction time from 1 minute to 10 minutes indicates an increasingly falling and rising absorbance price. This suggests that the stability of the Fe-APDC complex compound only occurs in a relatively short time. From this study obtained the optimum extraction time of 5 minutes. The increasing extraction time has an impact on the number of contacts between APDC and metal ions increasing, so that the number of complexes that occur is also increasing (Fallah, *et al.*, 2013). The long extraction time has an impact on the number of extractions of Fe ions obtained is also getting higher. However, at a longer extraction time after the optimum time is reached, it will not increase the number of percent extraction because by that time all the active groups of the ligand have bound to the Metal Ions of Fe (Yanti, 2019).

Analysis of XRF, XRD, and FTIR Diffractogram Red Mud

The extracted iron oxide powder was further analyzed using X-ray fluorescence (XRF). The results of the XRF red mud analysis after extraction with optimum conditions resulted in a change in the relative weight composition of the constituent elements contained in the red mud. The results of the XRF red mud analysis of the extraction results are shown in table 1.

Table 1. Red mud composition of XRF analysis results

Element	%Relative weight		Oxide compounds	%Relative weight	
	Before extraction	After Extraction		Before extraction	After Extraction
Fe	42.443%	62.443%	Fe_2O_3	30.448%	60.448%
Al	23.996%	10.096%	Al_2O_3	30.168%	10.268%
Si	23.014%	10.914%	SiO_2	30.748%	10.148%
Ti	3.175%	10.175%	Ti	1.747%	11.747%
Ca	2.182%	2.182%	CaO	1.728%	1.728%
Mg	1.366%	1.366%	MgO	1.558%	1.558%

The main difference of the extracted powder is the increase in fe elements in the red mud. This is because it is influenced by the extraction process using ammonium pyrolydine dithiocarbamate Ligand (APDC) which can be used for the extraction of kemite metals in organic solvents of methyl iso butyl ketone (MIBK), so that the Fe element contained in the sample increases. The element Fe which increases due to one of the properties of ferrous metals is an element of the transition group where one of the properties of the element of the transition group can form complex compounds of a specific color. The elemental composition of iron increased almost 2 times, followed by an increase in the element Ti in the red mud of the extraction results. This is thought to be due to the fairly strong bonding of Ti minerals with iron minerals in the form of Fe_2O_3-TiO_2 which are stabilized by the calcination process. The content of silica and alumina is seen to predominate in the form of oxide compounds indicating high levels of silica in red mud. Bauxite ore originating from Tayan, West Kalimantan, is reported to be classified as gibsite bauxite containing gibsit, quartz and kaolinite (Badmus, *et al.*, 2007).

The red mud extraction results were carried out XRD testing to identify the crystalline phase in the material by determining the parameters of the lattice structure and to obtain the particle size. XRD analysis was performed by comparing the control's Fe_2O_3 with the extraction resulted Fe_2O_3 shown in Figure 4.

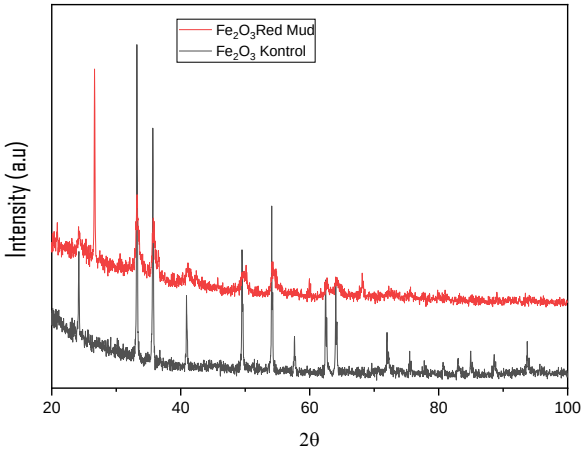

Figure 4. Analysis of XRD Fe_2O_3 control and Fe_2O_3 red mud

The analysis was carried out using the technique of synchronizing the results of experiments and controls. Analysis of XRD Fe_2O_3 extraction results from red mud showed that the dominant phase was hematite (Fe_2O_3) followed by the minor phase of SiO_2. If the peak diffraction profile is compared between the XRD test results on the red mud Fe_2O_3 sample and the control Fe_2O_3 defined by the hematite separation process, it shows that the diffraction peak is still sharp. The sharper the peak and the smaller the area, the higher the crystal quality of the synthesis result (Pailit, 2020). This is evidenced by the results of the analysis where the highest peak value (I / I0) is found in the SiO_2 compound with a value of 1000.00 with an FWHM value of 0.1050. SiO_2 compounds that appear according to the content of red mud can be seen in table 1. The mineral oxide has been confirmed to be compatible with the inorganic crystal structure database (ICSD) 98-004-1476 quartz low (SiO_2).

The less uniform FWHM Fe_2O_3 red mud value is evidenced by a sharp diffraction (peak) and only 4 peaks. This is thought to be due to the agglomeration process of Fe_2O_3 content in red mud when the extraction process is continued by calcination. The agglomeration occurs due to the relatively slow diffusion speed of HCl, causing the possibility of crystals to coagulate and rearrangement occurs which causes the pores to get smaller. The pores in the crystals will shrink gradually for a smaller pore size, so that the particles of hematite iron oxide (Fe_2O_3) undergo clumping (Byarappa, 2007).

The results of the XRD analysis of the comparison between Fe_2O_3 red mud and Fe_2O_3 control were then carried out further analysis using FTIR to determine the functional groups contained in the material and to identify the type of iron oxide formed. The results of the FTIR analysis are shown in figure 5.

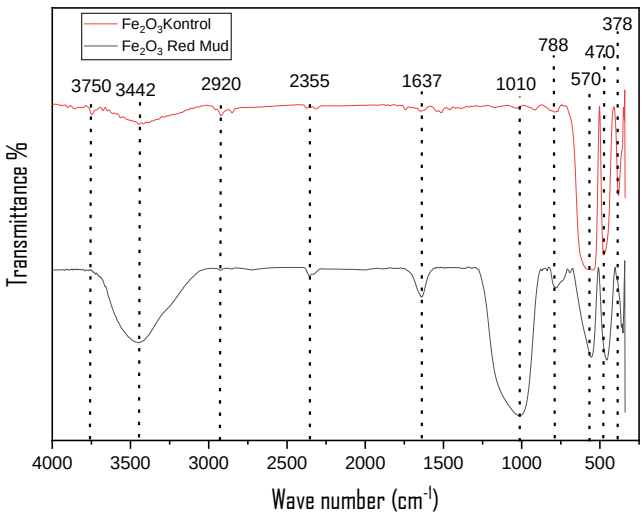

Figure 5. Analysis of FTIR Fe_2O_3 control and Fe_2O_3 red mud

The infrared spectrum (FTIR) of the red mud Fe_2O_3 nanoparticle is in the range of wave number 339.47-3448.72 cm^{-1} which identifies the chemical bonds as well as functional groups in the compound. Hematite (Fe_2O_3) extracted from red mud there is a strong wave number below 800 cm^{-1} which means that compounds other than hematite (Fe_2O_3) are identified. The large broad band at 3448.72 cm^{-1} is the O-H vibration of Fe-OH and Si-OH (Byarappa, 2007). The appearance of the vibration of the O-H group from Si-OH indicates that in Fe_2O_3 red mud the result of this extrasion there is silica. Silica appeared in Fe_2O_3 material from red mud extraction also supported by the emergence of peaks at wave numbers at peaks of 1014 cm^{-1} which is a characteristic absorption for Si-O vibration (asymmetrical ulcer) of the Si-O-Si group (siloxan) (Karbeka, 2020). The results of FTIR Fe_2O_3 red mud extraction results are correlated with XRD analysis which states that there is a SiO^2 peak. The existence of peak widening indicates an increasing number of functional groups (Senff, *et al*., 2011). The results of the FTIR analysis showed the presence of Fe-O stretching hematite phase (Fe_2O_3). IR bands at 869.90, 837.11, and 779.24 cm^{-1} can be identified as quartz and hematite phases typical of the red mud spectrum (Karbeka, 2020). The uptake of 916 cm^{-1} iron sand (control) is characteristic of the typical wave number of FeOOH waves in geothite compounds (α-FeOOH) (Guanghui, *et al*., 2014). The presence of an absorption of 1172 cm^{-1} indicates that there is still a magnetite phase in iron sand (control) which is different from the red mud hematite FTIR (Fe_2O_3) results where the magnetite phase is not detected.

Conclusion

The extraction results showed the formation of Fe_2O_3 compounds at optimum conditions (angles 2θ = 24.2327, 33.2376, 35.7572, 41.0323, 54.2710, 62.6731, 64.1030, 75.6129), SiO_2 (angle 2θ = 26.6162, 42.4372, 59.9820, 68.1830) due to calcination which resulted in a fairly strong bond of Si minerals with iron minerals. The Fe_2O_3 compound is formed due to the decomposition of the crystalline iron structure into amorphous, making it easier in the extraction process at optimum conditions. The calcination process was not affect the size of the iron oxide crystals produced, but affects the type of crystal phase formed.

References

Ardau, C., Lattanzi, P., Peretti, R., & Zucca, A. (2013). Treatment of Mine Wastes with Transformed Red Muds (TRM) and Other Iron Compounds: Leaching Column Tests. *Procedia Earth and Planetary Science*, *7*, 467–470.

Badmus, M. A. O., Audu, T. O. K., & Anyata, B. U. (2007). Removal of copper from industrial wastewaters by activated carbon prepared from periwinkle shells. *Korean Journal of Chemical Engineering*, *24*, 246–252.

Byrappa, K., & Adschiri, T. (2007). Hydrothermal technology for nanotechnology. *Progress in Crystal Growth and Characterization of Materials*, *53*(2), 117–166.

Fallah, A. A., Nematollahi, A., & Saei-Dehkordi, S. S. (2013a). Proximate composition and fatty acid profile of edible tissues of Capoeta damascina (Valenciennes, 1842) reared in freshwater and brackish water. *Journal of Food Composition and Analysis*, *32*(2), 150–154.

He, J., Jie, Y., Zhang, J., Yu, Y., & Zhang, G. (2013). Synthesis and characterization of red mud and rice husk ash-based geopolymer composites. *Cement and Concrete Composites*, *37*, 108–118.

Karbeka, M., & Nuryono, N. (2020). *Synthesis of silica coated on iron sand magnetic materials modified with 2-mercaptobenzimidazole through sol-gel*. 44–52.

Kansal, S. K., Sood, S., Umar, A., & Mehta, S. K. (2013). Photocatalytic degradation of Eriochrome Black T dye using well-crystalline anatase TiO2 nanoparticles. *Journal of Alloys and Compounds*, *581*, 392–397.

Li, G., Liu, M., Rao, M., Jiang, T., Zhuang, J., & Zhang, Y. (2014). Stepwise extraction of valuable components from red mud based on reductive roasting with sodium salts. *Journal of Hazardous Materials*, *280*, 774–780.

Lymperopoulou, T., Georgiou, P., Tsakanika, L. A., Hatzilyberis, K., & Ochsenkühn-Petropoulou, M. (2019). Optimizing Conditions for Scandium Extraction from Bauxite Residue Using Taguchi Methodology. *Minerals*, *9*, 236.

Nurhayani, F., Wulandari, A., & Suharsi, T. (2019). The Floral Morphology and Anatomy of Kenanga (Cananga odorata (Lam.) Hook.f. & Thomson). *IOP Conference Series: Earth and Environmental Science*, *394*, 012034.

Palit, C., & Suliestyah, S. (2020). Studi Konsentrasi Pada Bauksit Asal Tayan Dengan Menggunakan Metode Flotasi Kebalikan. *Jurnal Geomine*.

Rayaroth, M. P., Aravindakumar, C. T., Shah, N. S., & Boczkaj, G. (2022). Advanced oxidation processes (AOPs) based wastewater treatment - unexpected nitration side reactions - a serious environmental issue: A review. *Chemical Engineering Journal*, *430*, 133002.

Reid, S., Tam, J., Yang, M., & Azimi, G. (2017). Technospheric Mining of Rare Earth Elements from Bauxite Residue (Red Mud): Process Optimization, Kinetic Investigation, and Microwave Pretreatment. *Scientific Reports*, *7*.

Renforth, P., Mayes, W. M., Jarvis, A. P., Burke, I. T., Manning, D. A. C., & Gruiz, K. (2012). Contaminant mobility and carbon sequestration downstream of the Ajka (Hungary) red mud spill: The effects of gypsum dosing. *Science of The Total Environment*, *421–422*, 253–259.

Samal, S. (2021). Utilization of Red Mud as a Source for Metal Ions—A Review. *Materials*, *14*(9).

Senff, L., Hotza, D., & Labrincha, J. A. (2011). Effect of red mud addition on the rheological behaviour and on hardened state characteristics of cement mortars. *Construction and Building Materials*, *25*, 163–170.

Singh, S., Aswath, M. U., das Biswas, R., Ranganath, R. v, Choudhary, H. K., Kumar, R., & Sahoo, B. (2019). Role of iron in the enhanced reactivity of pulverized Red mud: Analysis by Mössbauer spectroscopy and FTIR spectroscopy. *Case Studies in Construction Materials*, *11*, e00266.

Yanti, E., & Patrisia, D. (2019). The impact of Corporate Governance Mechanisms on Firm Value. *Proceedings of the Third Padang International Conference On Economics Education, Economics, Business and Management, Accounting and Entrepreneurship (PICEEBA 2019)*, 242–249.

Ye, N., Chen, Y., Yang, J., Liang, S., Hu, Y., Hu, J., Zhu, S., Fan, W., & Xiao, B. (2017). Transformations of Na, Al, Si and Fe species in red mud during synthesis of one-part geopolymers. *Cement and Concrete Research*, *101*, 123–130.